

BRIEF REPORT

In Vivo ^{18}F -Florzolotau Tau Positron Emission Tomography Imaging in Parkinson's Disease Dementia

Yilin Tang, MD,¹ Ling Li, PhD,² Tianyu Hu, MD,¹ Fangyang Jiao, PhD,³ Linlin Han, PhD,¹ Shiyu Li, MD,¹ Zhiheng Xu, MD,¹ Yun Fan, PhD,¹ Yimin Sun, PhD,¹ Fengtao Liu, MD,¹ Tzu-Chen Yen, MD, PhD,⁴ Chuantao Zuo, MD, PhD,^{2*} and Jian Wang, MD, PhD^{1*}

¹Department of Neurology and National Research Center for Aging and Medicine and National Center for Neurological Disorders, State Key Laboratory of Medical Neurobiology, Huashan Hospital, Fudan University, Shanghai, China ²Department of Nuclear Medicine, Zhongnan Hospital of Wuhan University, Wuhan University, Wuhan, China ³PET Center, Huashan Hospital, Fudan University, Shanghai, China ⁴APRINOIA Therapeutics Co., Ltd, Suzhou, China

ABSTRACT: **Background:** Tau pathology is observed during autopsy in many patients with Parkinson's disease dementia (PDD). Positron emission tomography (PET) imaging using the tracer ^{18}F -florzolotau has the potential to capture tau accumulation in the living brain.

Objective: The aim was to describe the results of ^{18}F -florzolotau PET/CT (computed tomography) imaging in patients with PDD.

***Correspondence to:** Prof. Jian Wang, Department of Neurology, Huashan Hospital, Fudan University, 12 Wulumuqi Zhong Road, Shanghai 200040, China; E-mail: wangjian_hs@fudan.edu.cn OR Prof. Chuantao Zuo, PET Center, Huashan Hospital, Fudan University, 518 East Wuzhong Road, Shanghai 200235, China; E-mail: zuochuantao@fudan.edu.cn

Relevant conflicts of interest/financial disclosures: Tzu-Chen Yen is an employee of APRINOIA Therapeutics Co., Ltd, Suzhou, China. All other authors declare that they have no conflicts of interest.

Funding agencies: This work was financially supported by the Shanghai Municipal Science and Technology Major Project (grants 2018SHZDZX01 and 21S31902200 to J.W.), the National Health Commission of China (grant Pro20211231084249000238 to J.W.), the National Natural Science Foundation of China (grants 82171421 and 91949118 to J.W.; grants 82021002, 81971641, and 81671239 to C.Z.), the Research Project of the Shanghai Health Commission (grant 2020YJZX0111 to C.Z.), and the Clinical Research Plan of SHDC (grant SHDC2020CR1038B to C.Z.).

Yilin Tang, Ling Li, and Tianyu Hu are contributed equally to this work. Chuantao Zuo and Jian Wang jointly supervised the work.

Received: 29 June 2022; **Revised:** 19 October 2022; **Accepted:** 30 October 2022

Published online in Wiley Online Library
(wileyonlinelibrary.com). DOI: 10.1002/mds.29273

Methods: Ten patients with PDD, 9 with Parkinson's disease with normal cognition (PD-NC), and 9 age-matched healthy controls (HCs) were enrolled. Clinical assessments and ^{18}F -florzolotau PET/CT imaging were performed.

Results: ^{18}F -Florzolotau uptake was significantly higher in the cortical regions of patients with PDD compared with both PD-NC and HCs, especially in the temporal lobe. Notably, ^{18}F -florzolotau uptake in the occipital lobe of patients with PDD showed a significant correlation with cognitive impairment as reflected by Mini-Mental State Examination (MMSE) scores.

Conclusions: ^{18}F -Florzolotau PET imaging can effectively capture the occurrence of tau pathology in patients with PDD, which was also linked to MMSE scores. © 2022 International Parkinson and Movement Disorder Society.

Key Words: Parkinson's disease dementia; ^{18}F -florzolotau; tau PET imaging

The long-term clinical course of Parkinson's disease (PD) is complicated by the onset of dementia in 80% of patients.¹ However, the pathogenesis of PD dementia (PDD) is complex and has not been fully elucidated. Although α -synuclein deposition is traditionally considered as the key pathological hallmark of PD,²⁻⁴ several autopsy studies found evidence of tau pathology in PDD brains.⁵⁻⁷ Nonetheless, the proportion of patients showing moderate-to-severe tau accumulation varied markedly (from 30% to 97%) in previous *postmortem* studies.⁸⁻¹⁰

In recent years, there has been growing interest in tracking tau pathology using PET. Previous studies reported an increased uptake of the first-generation tau tracer ^{18}F -AV-1451 in the temporal and parietal cortex of patients with PD with cognitive impairment.^{11,12} Unfortunately, traditional tau PET tracers are limited by off-target binding^{13,14} and/or the inability to capture the distribution patterns of tau pathology in non-Alzheimer's disease (AD) tauopathies.^{15,16} Recently, several studies have described the clinical utility of the second-generation tau tracer ^{18}F -florzolotau (previously known as ^{18}F -APN-1607 or ^{18}F -PM-PBB3) for the detection of tau pathology in the living brain of patients with AD¹⁷⁻¹⁹ and other neurodegenerative diseases, including progressive supranuclear palsy,²⁰ multiple system atrophy-parkinsonian subtype,²¹ and frontotemporal lobar degeneration with tauopathy due to MAPT mutations.²² Different from first-generation tau PET tracers, ^{18}F -florzolotau is characterized by an

elevated signal-to-noise ratio and limited off-target binding.¹⁷ However, the question whether ¹⁸F-florazolotau PET/CT (computed tomography) might have value in patients with PDD remains unanswered. This cross-sectional study was therefore designed to address this issue. Based on previous neuropathological observations, we hypothesized that ¹⁸F-florazolotau uptake would be higher in patients with PDD compared with both patients with PD with normal cognition (PD-NC) and cognitively healthy controls (HCs). A significant heterogeneity in terms of tau deposition was also expected in patients with PDD.

Patients and Methods

Participants

All visits and procedures occurred at the Movement Disorders Clinic, Department of Neurology, Huashan Hospital, Fudan University. Enrollment started in November 2019 and concluded in April 2021. The study sample consisted of 10 patients with PDD, 9 with PD-NC, and 9 age-matched cognitively HCs with no history of neurological or psychiatric disorders. PD was diagnosed according to the Movement Disorder Society Clinical Criteria.²³ The study was conducted in accordance with the Declaration of Helsinki, and the protocol was approved by the Institutional Review Board of the Huashan Hospital (approval number: 2019-433). All participants or legal guardians provided written informed consent.

Clinical and Neuropsychological Evaluation

A detailed description of the clinical and neuropsychological evaluation is provided in the Supplementary Materials in Appendix S1.

Image Acquisition

A detailed description of the image acquisition is provided in the Supplementary Materials in Appendix S1.

Image Processing

Individual PET and corresponding T1-weighted MRI images were coregistered using the SPM12 software (<http://www.fil.ion.ucl.ac.uk/spm/software/spm12/>) implemented in MATLAB 9.5 (MathWorks, Natick, MA, USA). The transformation matrices of segmented T1-weighted magnetic resonance imaging (MRI) were applied to matched PET images into the Montreal Neurological Institute standard space. We applied a partial volume correction using a segmented gray matter mask and the Muller-Gartner method.²³ MRI-coregistered PET scans were spatially normalized using subject-specific transformation matrixes obtained from MRI. Images were subsequently smoothed using a Gaussian

kernel (full-width at half-maximum: 6 mm). The cerebellar gray matter (with the exclusion of the deep nucleus) was chosen as the reference region to obtain standardized uptake value ratio (SUVR) maps.^{17,24} Mean regional SUV values were extracted from the following regions of interest (ROIs): frontal cortex, parietal cortex, occipital cortex, temporal cortex, hippocampus, insula, caudate, and putamen. All regions were identified from the automated anatomical atlas three template and the Wake Forest University PickAtlas (version 3.0). Values extracted from bilateral ROIs were used in subsequent analyses. ¹⁸F-Florazolotau SUV maps obtained in three study groups were compared in a voxel-wise fashion using 2-tailed Student's *t* tests. The voxel-level threshold was set to an uncorrected *P*-value <0.001. All procedures were carried out using Statistical Parametric Mapping (SPM).

Data Analysis

The statistical methods are described in the Supplementary Materials in Appendix S1.

Results

General Characteristics

Table 1 and Table S1 in Appendix S1 present the general characteristics of the three study groups (PDD, PD-NC, and HCs).

Regional ¹⁸F-Florazolotau Uptake

Quantitative measures of ¹⁸F-florazolotau uptake in the three study groups are presented in Table 1. Compared with both patients with PD-NC and HCs, those with PDD showed a significantly higher ¹⁸F-florazolotau binding in the following regions: frontal, parietal, occipital, temporal, and insula lobes and putamen. ¹⁸F-Florazolotau uptake in patients with PD-NC did not differ significantly from that observed in HCs. Quantitative measures of ¹⁸F-florazolotau uptake in the three study groups as well as a group of previously collected patients with AD¹⁹ are described in Appendix S1.

Regions showing significant intergroup differences are summarized in Figure 1 and Table S1 in Appendix S1. The results of SPM analysis revealed that patients with PDD had a higher cortical ¹⁸F-florazolotau uptake compared with both patients with PD-NC and HCs; this was especially evident for the temporal lobe (uncorrected *P*-value <0.001). Individual ¹⁸F-florazolotau binding data are shown in Figure S1 in Appendix S1, whereas Figure 1D shows a heat map of regional ¹⁸F-florazolotau uptake. On visual inspection, more than 50% of patients with PDD showed an increased tau accumulation in the cortical regions; however, very mild or absent ¹⁸F-florazolotau uptake was

TABLE 1 Clinical characteristics of the study participants and quantitative results of ¹⁸F-florzolotau binding at the group level

	PDD	PD-NC	HCs	PDD vs. PD-NC	PDD vs. HCs	PD-NC vs. HCs
Number of subjects	10	9	9			
Age (y) ^a	69.3 ± 5.4	69.2 ± 6.8	63.8 ± 3.6	1.000	0.109	0.131
Sex (men/women) ^b	8/2	6/3	4/5	0.510	0.109	0.343
Education (y) ^c	10.4 ± 3.8	10.6 ± 4.6	—	0.942	—	—
Disease duration (mo) ^c	34.9 ± 16.7	24.2 ± 17.5	—	0.192	—	—
MDS-UPDRS-III score ^c	45.1 ± 18.6	40.8 ± 17.6	—	0.685	—	—
Hoehn and Yahr stage ^c	2.4 ± 0.6	2.4 ± 0.5	—	0.914	—	—
LEDD (mg/d) ^c	378.4 ± 227.3	303.6 ± 293.1	—	0.603	—	—
GDS score ^c	9.8 ± 2.3	11.0 ± 10.0	—	0.786	—	—
MMSE score ^a	16.1 ± 5.7	26.5 ± 2.4	26.4 ± 3.0	<0.001	<0.001	1.000
MoCA score ^c	11.1 ± 6.2	25.7 ± 1.9	—	<0.001	—	—
SUVR ^a						
Frontal cortex	1.13 ± 0.39	0.73 ± 0.18	0.66 ± 0.08	0.007	0.002	1.000
Parietal cortex	1.14 ± 0.37	0.72 ± 0.16	0.67 ± 0.08	0.003	0.001	1.000
Occipital cortex	1.37 ± 0.44	0.93 ± 0.18	0.89 ± 0.11	0.008	0.004	1.000
Temporal cortex	1.46 ± 0.39	1.01 ± 0.22	0.94 ± 0.12	0.004	0.001	1.000
Hippocampus	1.48 ± 0.70	1.48 ± 0.71	1.54 ± 0.51	1.000	1.000	1.000
Insula	1.28 ± 0.42	0.85 ± 0.18	0.85 ± 0.13	0.010	0.009	1.000
Caudate	0.90 ± 0.40	0.73 ± 0.17	0.63 ± 0.08	0.505	0.106	1.000
Putamen	1.66 ± 0.51	1.15 ± 0.30	1.01 ± 0.18	0.015	0.002	1.000

Note: Data are expressed as means ± standard deviations.

Abbreviations: GDS, Geriatric Depression Scale; HCs, healthy controls; LEDD, levodopa equivalent daily dose; MDS-UPDRS, Movement Disorders Society Unified Parkinson's Disease Rating Scale; MMSE, Mini-Mental State Examination; MoCA, Montreal Cognitive Assessment; PDD, Parkinson's disease dementia; PD-NC, Parkinson's disease and normal cognition; SUVR, standardized uptake value ratio.

^aOne-way ANOVA followed by Bonferroni's post hoc correction for multiple comparisons.

^b χ^2 test.

^cStudent's *t* test.

observed in 3 patients with PDD (patient numbers 1, 7, and 10).

Correlations between ¹⁸F-Florzolotau Uptake and Cognitive Functioning

¹⁸F-Florzolotau uptake in the occipital lobe of patients with PDD showed a significant negative correlation with Mini-Mental State Examination (MMSE) scores ($R = -0.635$, $P = 0.0486$; Fig. S3 in Appendix S1). However, no association was observed for patients with PD-NC (Fig. S4 in Appendix S1).

Discussion

Our study addresses an evidence gap regarding the potential usefulness of ¹⁸F-florzolotau as a PET imaging biomarker of tau pathology in patients with PDD.

There are two principal findings from our investigation. First, we found that ¹⁸F-florzolotau binding in the cortical areas and putamen was significantly higher in patients with PDD compared with those with PD-NC and HCs. Second, ¹⁸F-florzolotau retention in the occipital lobe of patients with PDD was significantly associated with the severity of cognitive impairment as reflected by MMSE scores.

The occurrence of tau pathology in PDD brains has been previously reported on *postmortem* examinations.^{25,26} Early work with ¹⁸F-AV-1451 found an increased tracer uptake in the inferior temporal gyrus and precuneus of PD patients with cognitive impairment compared with HCs.¹¹ In another study focusing on PDD, Smith and colleagues¹² reported an elevated ¹⁸F-AV-1451 retention in the medial areas of the parietal lobe and the inferior temporal lobes. On examining the occurrence of tau pathology in the living PDD brain

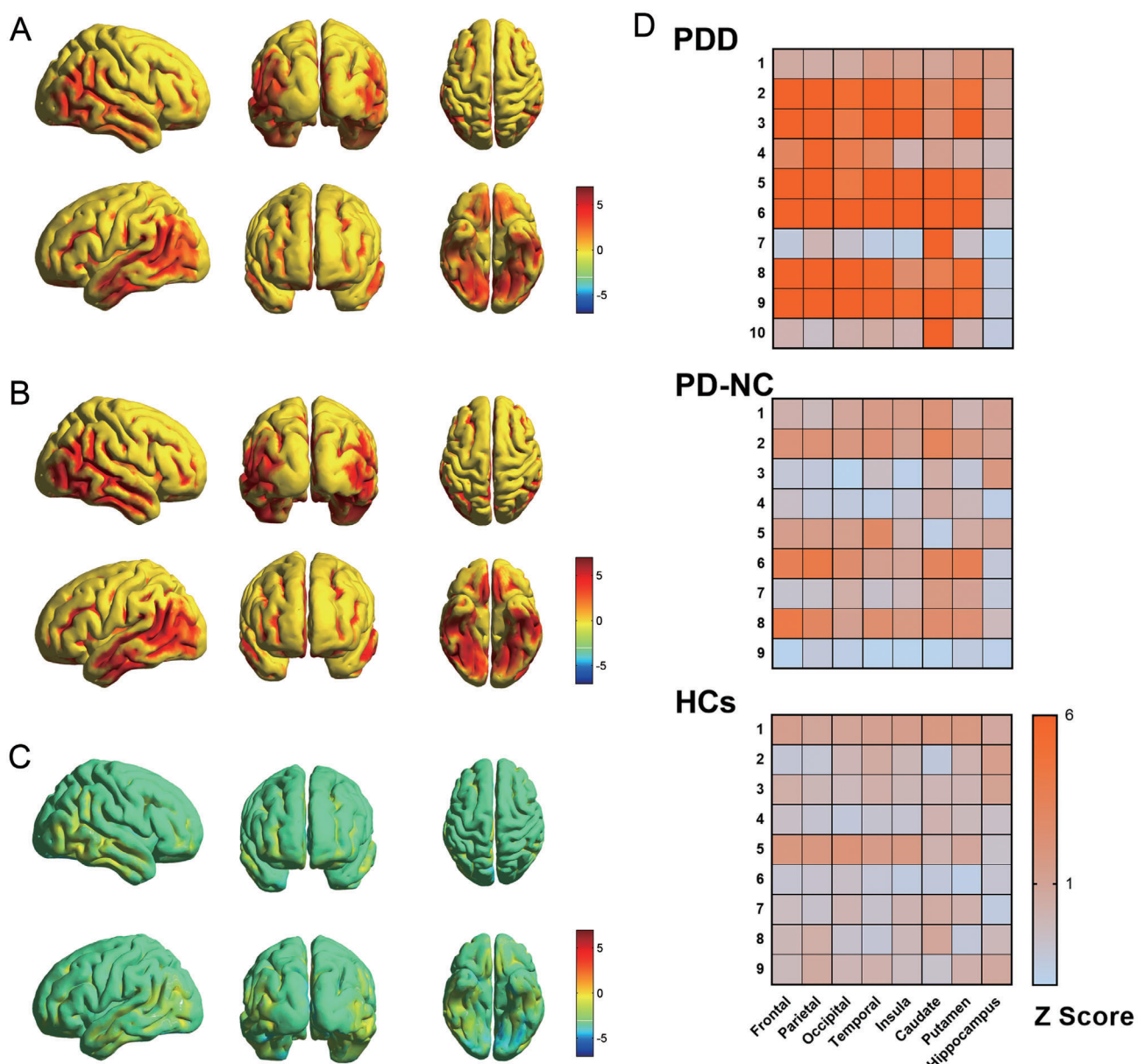


FIG. 1. Intergroup comparison of ^{18}F -florlzotau uptake values. The analysis was carried out using voxel-based statistical parametric mapping, with age and sex entered as covariates. ^{18}F -Florlzotau uptake is displayed on a single-subject MRI brain template using an uncorrected P -value of 0.001 as threshold. (A) PDD versus PD-NC; (B) PDD versus HCs; (C) PD-NC versus HCs; (D) patient-level heat map of regional z scores (individual ^{18}F -florlzotau PET imaging findings). HCs, healthy controls; MRI, magnetic resonance imaging; PDD, Parkinson's disease dementia; PD-NC, Parkinson's disease with normal cognition; PET, positron emission tomography. [Color figure can be viewed at wileyonlinelibrary.com]

using ^{18}F -florlzotau, we found that the patterns of tracer uptake were more widespread than that previously reported for first-generation tau PET probes; accordingly, an involvement of the frontal, parietal, temporal, and occipital regions was observed in our study. This apparent discrepancy may be partially explained by the intrinsic properties of ^{18}F -florlzotau, including a high affinity for 4-repeat tau isoforms and an elevated signal-to-noise ratio.¹⁷ The relatively severe cognitive impairment observed in our patients with PDD may also account for the more widespread tracer

retention, a plausible explanation for the negative correlation between MMSE scores and ^{18}F -florlzotau uptake in the occipital lobe. Therefore, larger impairments were observed in MMSE among our patients with PDD (mean score: 16.1 ± 5.7) compared with previous studies conducted with ^{18}F -AV-1451 (mean scores: 24.9 ± 1.5 ¹¹ and 22.0 ± 4.0).¹² Although more than 50% of our patients with PDD showed an increased tau accumulation in cortical regions, very mild or no ^{18}F -florlzotau uptake was observed in three patients. This may be due to a limited burden of

cortical tau deposition that was below the detection threshold during ¹⁸F-florzolotau PET imaging. This should not come as a surprise, as PDD is a pathologically heterogeneous disorder and an increased tau burden is not invariably present.^{3,27,28} Although positive ¹⁸F-florzolotau findings may be useful to confirm the presence of an underlying tau pathology, negative results when strict clinical diagnostic criteria are applied should prompt a thorough follow-up schedule. Our study also adds to the literature by describing an inverse association between ¹⁸F-florzolotau uptake in the occipital lobe of patients with PDD and MMSE scores. Whether tau PET imaging findings can be related to the severity of cognitive impairment in patients with PD remains unclear. Prior work with ¹⁸F-AV-1451 yielded inconsistent findings, with some,^{11,12} but not all,²⁹ studies reporting a positive association with the extent of tracer retention and the degree of cognitive deterioration. Although statistically significant, the correlation between ¹⁸F-florzolotau uptake and MMSE scores observed in our study was modest. It can be expected that the heterogeneity of PDD will continue to challenge the development of robust imaging biomarkers to reflect disease severity. Additional prospective studies are required to identify optimal approaches to characterizing disease severity with tau PET imaging, particularly with respect to the association between ¹⁸F-florzolotau uptake and longitudinal trajectories of cognitive deterioration.

Several limitations to this study are worth noting. First, tau hyperphosphorylation is a common feature between AD and PDD.^{3,25} Unfortunately, the limited availability of plasma samples in our study precluded an evaluation of both AD-related tau biochemical markers (ie, elevated levels of total tau and tau hyperphosphorylated tau at threonine 181 [p -tau₁₈₁]) and amyloid β -related proteins. As we had no data concerning biomarkers, we were unable to stratify the study participants for the concomitant presence of AD pathology.⁸ In addition, in an effort to reduce radiation exposure, we did not track AD-related pathology using amyloid-specific PET tracers. However, the diagnosis of PDD was confirmed by applying both strict clinical diagnostic criteria (2007 MDS) and dopaminergic PET imaging (Fig. S5 in Appendix S1). Second, the sample size may not have been sufficiently large to identify other potential differences in the three groups, and larger cohorts are required to confirm our findings. Third, because of the cross-sectional design, the observed association between ¹⁸F-florzolotau uptake and MMSE scores should not be interpreted as a causal effect. Fourth, regional SUVR values utilized in the analysis might not accurately reflect the burden of tau accumulation within each ROI. Finally, it would have been interesting to use a dynamic PET acquisition protocol to minimize the effect of blood flow; however, as we were unable to implement this approach, we addressed this

potential confounder by applying the technique described by Tagai and colleagues.¹⁷

Conclusions

¹⁸F-Florzolotau PET imaging can effectively capture the occurrence of tau pathology in patients with PDD, which was also linked to MMSE scores. ■

Acknowledgments: We thank all patients and controls involved in this research. We are grateful to APRINOIA Therapeutics for providing the tosylate precursor used for ¹⁸F-florzolotau radiosynthesis.

Data Availability Statement

The datasets generated during and/or analyzed during the current study are available from the corresponding author on reasonable request.

References

1. Hely MA, Reid WGJ, Adena MA, Halliday GA, Morris JGL. The Sydney multicenter study of Parkinson's disease: the inevitability of dementia at 20 years. *Movement Disord* 2008;23(6):837–844.
2. Aarsland D, Perry R, Brown A, Larsen JP, Ballard C. Neuropathology of dementia in Parkinson's disease: a prospective, community-based study. *Ann Neurol* 2005;58(5):773–776.
3. Irwin DJ, White MT, Toledo JB, et al. Neuropathologic substrates of Parkinson disease dementia. *Ann Neurol* 2012;72(4):587–598.
4. Braak H, Rub U, Jansen Steur EN, Del Tredici K, de Vos RA. Cognitive status correlates with neuropathologic stage in Parkinson disease. *Neurology* 2005;64(8):1404–1410.
5. Coughlin D, Xie SX, Liang M, et al. Cognitive and pathological influences of tau pathology in Lewy body disorders. *Ann Neurol* 2019;85(2):259–271.
6. Halliday G, Hely M, Reid W, Morris J. The progression of pathology in longitudinally followed patients with Parkinson's disease. *Acta Neuropathol* 2008;115(4):409–415.
7. Irwin DJ, Grossman M, Weintraub D, et al. Neuropathological and genetic correlates of survival and dementia onset in synucleinopathies: a retrospective analysis. *Lancet Neurol* 2017;16(1):55–65.
8. Smith C, Malek N, Grosset K, Cullen B, Gentleman S, Grosset DG. Neuropathology of dementia in patients with Parkinson's disease: a systematic review of autopsy studies. *J Neurol Neurosurg Psychiatry* 2019;90(11):1234–1243.
9. Horvath J, Herrmann FR, Burkhard PR, Bouras C, Kovari E. Neuropathology of dementia in a large cohort of patients with Parkinson's disease. *Parkinsonism Relat Disord* 2013;19(10):864–868, discussion 864.
10. Jellinger KA, Seppi K, Wenning GK, Poewe W. Impact of coexistent Alzheimer pathology on the natural history of Parkinson's disease. *J Neural Transm* 2002;109(3):329–339.
11. Gomperts SN, Locascio JJ, Makarets SJ, et al. Tau positron emission tomographic imaging in the Lewy body diseases. *JAMA Neurol* 2016;73(11):1334–1341.
12. Smith R, Scholl M, Londos E, Ohlsson T, Hansson O. ¹⁸F-AV-1451 in Parkinson's disease with and without dementia and in dementia with Lewy bodies. *Sci Rep* 2018;8(1):4717.
13. Marquie M, Verwer EE, Meltzer AC, et al. Lessons learned about ^[F-18]-AV-1451 off-target binding from an autopsy-confirmed Parkinson's case. *Acta Neuropathol Commun* 2017;5(1):75.
14. Bevan-Jones WR, Cope TE, Jones PS, et al. ^{[18]F}AV-1451 binding in vivo mirrors the expected distribution of TDP-43 pathology in

- the semantic variant of primary progressive aphasia. *J Neurol Neurosurg Psychiatry* 2018;89(10):1032–1037.
15. Schonhaut DR, McMillan CT, Spina S, et al. (18) F-flortaucipir tau positron emission tomography distinguishes established progressive supranuclear palsy from controls and Parkinson disease: a multicenter study. *Ann Neurol* 2017;82(4):622–634.
 16. Jones DT, Knopman DS, Graff-Radford J, et al. In vivo (18)F-AV-1451 tau PET signal in MAPT mutation carriers varies by expected tau isoforms. *Neurology* 2018;90(11):e947–e954.
 17. Tagai K, Ono M, Kubota M, et al. High-contrast In vivo imaging of tau pathologies in Alzheimer's and non-Alzheimer's disease Tauopathies. *Neuron* 2021;109(1):42–58 e48.
 18. Hsu JL, Lin KJ, Hsiao IT, et al. The imaging features and clinical associations of a novel tau PET tracer-18F-APN1607 in Alzheimer disease. *Clin Nucl Med* 2020;45(10):747–756.
 19. Lu J, Bao W, Li M, et al. Associations of [(18)F]-APN-1607 tau PET binding in the brain of Alzheimer's disease patients with cognition and glucose metabolism. *Front Neurosci* 2020;14:604.
 20. Li L, Liu FT, Li M, et al. Clinical utility of (18) F-APN-1607 tau PET imaging in patients with progressive Supranuclear palsy. *Mov Disord* 2021;36(10):2314–2323.
 21. Liu FT, Li XY, Lu JY, et al. (18) F-Florzolotau tau positron emission tomography imaging in patients with multiple system atrophy-parkinsonian subtype. *Mov Disord* 2022;37(9):1915–1923.
 22. Zhou XY, Lu JY, Liu FT, et al. In vivo (18) F-APN-1607 tau positron emission tomography imaging in MAPT mutations: cross-sectional and longitudinal findings. *Mov Disord* 2022;37(3):525–534.
 23. Postuma RB, Berg D, Stern M, et al. MDS clinical diagnostic criteria for Parkinson's disease. *Mov Disord* 2015;30(12):1591–1601.
 24. Brendel M, Barthel H, van Eimeren T, et al. Assessment of 18F-PI-2620 as a biomarker in progressive Supranuclear palsy. *JAMA Neurol* 2020;77(11):1408–1419.
 25. Compta Y, Parkkinen L, O'Sullivan SS, et al. Lewy- and Alzheimer-type pathologies in Parkinson's disease dementia: which is more important? *Brain* 2011;134(Pt 5):1493–1505.
 26. Irwin DJ, Lee VM, Trojanowski JQ. Parkinson's disease dementia: convergence of alpha-synuclein, tau and amyloid-beta pathologies. *Nat Rev Neurosci* 2013;14(9):626–636.
 27. Hughes AJ, Daniel SE, Blankson S, Lees AJ. A clinicopathologic study of 100 cases of Parkinson's disease. *Arch Neurol* 1993;50(2):140–148.
 28. Sabbagh MN, Adler CH, Lahti TJ, et al. Parkinson disease with dementia: comparing patients with and without Alzheimer pathology. *Alzheimer Dis Assoc Discord* 2009;23(3):295–297.
 29. Hansen AK, Damholdt MF, Fedorova TD, et al. In vivo cortical tau in Parkinson's disease using 18F-AV-1451 positron emission tomography. *Mov Disord* 2017;32(6):922–927.

Supporting Data

Additional Supporting Information may be found in the online version of this article at the publisher's web-site.

SGML and CITI Use Only
DO NOT PRINT

Author Roles

- (1) Research project: A. Conception, B. Organization, C. Execution;
(2) Statistical Analysis: A. Design, B. Execution, C. Critical revision;
(3) Manuscript: A. Draft writing, B. Critical revision.

Y.T.: 1A, 1B, 1C, 2A, 2B, 2C, 3A, 3B

L.L.: 1A, 1B, 1C, 2A, 2B, 2C, 3A, 3B

T.H.: 1A, 1B, 1C, 2A, 2B, 2C, 3A, 3B

F.J.: 1C, 2B, 2C, 3B

L.H.: 1C, 2B, 2C, 3B

S.L.: 1C, 2B, 2C, 3B

Z.X.: 1C, 2B, 2C, 3B

Y.F.: 1C, 2B, 2C, 3B

Y.S.: 1C, 2B, 2C, 3B

F.L.: 1C, 2B, 2C, 3B

T.-C.Y: 1C, 2B, 2C, 3B

C.Z.: 1A, 1B, 2A, 2B, 2C, 3A, 3B

J.W.: 1A, 1B, 2A, 2B, 2C, 3A, 3B